Temperature dependent low energy electron microscopy study of Ge island growth on bare and Ga terminated Si(112)

2009 J. Phys.: Condens. Matter 21 314020

(http://iopscience.iop.org/0953-8984/21/31/314020)

J. Phys.: Condens. Matter **21** (2009) 314020 (7pp) doi:10.1088/0953-8984/21/31/314020

Temperature dependent low energy electron microscopy study of Ge island growth on bare and Ga terminated Si(112)

M Speckmann[1], Th Schmidt[1], J I Flege[1,2], J T Sadowski[2], P Sutter[2] and J Falta[1]

[1] Institute of Solid State Physics, University of Bremen, Otto-Hahn-Allee 1, 28359 Bremen, Germany
[2] Center for Functional Nanomaterials, Brookhaven National Laboratory, Upton, NY 11973, USA

E-mail: mspeckmann@ifp.uni-bremen.de

Received 30 December 2008, in final form 18 May 2009
Published 7 July 2009
Online at stacks.iop.org/JPhysCM/21/314020

Abstract

The pre-adsorption of Ga on Si(112) leads to a drastic change of the morphology of subsequently grown Ge islands. In contrast to the case for Ge growth on bare Si(112), even nanowire growth can be achieved on Ga terminated Si(112). Employing low energy electron microscopy and low energy electron diffraction, the initial phase of Ge nucleation and Ge island growth was systematically analysed for growth temperatures between 420 and 610 °C, both on clean and on Ga terminated Si(112). In both cases the island density exhibits an Arrhenius-like behaviour, from which diffusion barrier heights of about 1.3 and 1.0 eV can be estimated for growth with and without Ga pre-adsorption, respectively. The Ge island shape on the bare Si(112) surface is found to be nearly circular over the whole temperature range, whereas the shapes of the Ge islands on the Ga terminated Si(112) become highly anisotropic for higher temperatures. Ge nanowires with sizes of up to 2 μm along the [1$\bar{1}$0] direction are observed.

(Some figures in this article are in colour only in the electronic version)

1. Introduction

The growth of germanium nanostructures on silicon substrates is a promising approach towards the production of high-speed devices, since it combines the higher carrier mobility and the smaller band gap of germanium with the well-established and cost-efficient silicon technology. Thus, this field is attracting a lot of interest in current research [1–4]. To change and influence the characteristic Stranski–Krastanov growth of Ge on Si [5] there are different methods, e.g., the use of graded buffer layers [6] or surfactants [7, 8], which allow for achieving the desired surface morphology like smooth two-dimensional layers [9–13] or enhanced three-dimensional island growth [14–16].

The high step densities of vicinal silicon substrates like the (112) surface may lead to advanced technological applications because of enhanced step flow and improved growth [17–19]. Due to the low symmetry of such substrates, the growth of highly anisotropic structures like Ge nanowires can be expected.

The clean Si(112) surface is unstable and, as a result, (111) and (337) facets appear. The self-organized growth of atom wires along the highly reactive step edges of these facets was already observed for Ga [20–22] and Al [23]. In this study we analysed the influence of the pre-adsorbed Ga on the growth of Ge islands by means of low energy electron microscopy (LEEM), low energy electron diffraction (LEED), x-ray photoemission microscopy (X-PEEM) and core level spectroscopy (CLS). In particular, we will focus on the temperature dependence of the Ge island growth and present a systematic study comparing the Ge growth on bare Si(112) and on the Ga terminated Si(112) surface.

2. Experimental details

All experiments of this study were performed under ultra-high vacuum (UHV) conditions with a base pressure in the low 10^{-10} mbar regime. The LEEM, X-PEEM, CLS and LEED data were taken at the beamline U5UA at the VUV-IR

storage ring of the National Synchrotron Light Source (NSLS) at the Brookhaven National Laboratory (BNL) in Upton, NY, USA [24]. The core level spectra were extracted from X-PEEM images that were taken at photon energies ranging from 120 to 145 eV.

The microscope employed for this study is a LEEM III by Elmitec GmbH. All images and spectra were processed with the programme Gxsm by Zahl *et al* [25].

After cutting from a silicon wafer and cleaning with methyl or ethyl alcohol the samples were degassed in UHV for at least 16 h at a temperature of about 600 °C. Subsequently the samples were flashed several times up to about 1200 °C for 30–60 s until the native oxide layer was completely removed and the LEED patterns obtained after cool-down clearly showed the expected reconstructions. The heating was performed with e-beam bombardment from the back side of the sample. The temperature was monitored with an infrared pyrometer and a thermocouple attached below the sample. Small amounts of Ge (a few monolayers), either with or without prior Ga adsorption, were deposited onto the Si(112) samples at temperatures in the range from 420 to 610 °C, using an electron beam evaporator (Omicron triple EFM). For Ge growth on Ga terminated Si(112), the Ga flux was maintained during Ge deposition.

The Ga and Ge exposures were estimated from the transition of the $(\sqrt{3} \times \sqrt{3})$-R30° to the (6.3 × 6.3) reconstruction and the transition of the (7 × 7) to the (5×5) structure on the Si(111) surface, respectively. The $(\sqrt{3} \times \sqrt{3})$-R30° structure is completely developed at a Ga coverage of exactly $\frac{1}{3}$ ML_{111} [26, 27], where 1 ML_{111} corresponds to 7.83×10^{14} atoms cm^{-2}, and the (5×5) structure is completed at a coverage of 4 ML_{111} [28]. The Ge flux was in the range of (0.18 ± 0.02) ML min^{-1}. Here and in the following we refer to a monolayer (ML) as the atom density of the bulk-terminated Si(112) surface, i.e. 1 ML = 5.54×10^{14} cm^{-2}. The preparation was monitored in situ with LEED or LEEM.

3. Results and discussion

3.1. Ge wetting layer formation on Si(112)

LEED patterns (cf figure 1) of the bare Si(112) surface exhibit spots at $\frac{n}{7}$ and $\frac{1}{2}$ of the surface Brillouin zone (SBZ) that are elongated along $[11\bar{1}]$ direction. Thus, the corresponding domains in real space are narrow in $[11\bar{1}]$ and large in the perpendicular $[1\bar{1}0]$ direction. In agreement with literature [29–31] we assign these spots to (7 × 7) reconstructed (111) facets [32] and (2 × 1) reconstructed (337) facets [33].

In figure 2(a) a LEEM image of such a bare Si(112) surface is depicted. A faint contrast with stripes along $[1\bar{1}0]$ can be observed. As the expected width of the facets (⩽13 nm [29]) is below the resolution limit of the microscope (≈40 nm), it is not clear whether these stripes correspond to individual facets or, e.g., to step bunches. In any case, a contrast with preferential direction from the lower right to the upper left is obvious. After deposition of around 1 ML of Ge onto this surface the contrast in the LEEM image (cf figure 2(b)) vanishes completely. This can be attributed to a change in the surface structure and/or the roughening of the step edges due to the formation of a Ge wetting layer.

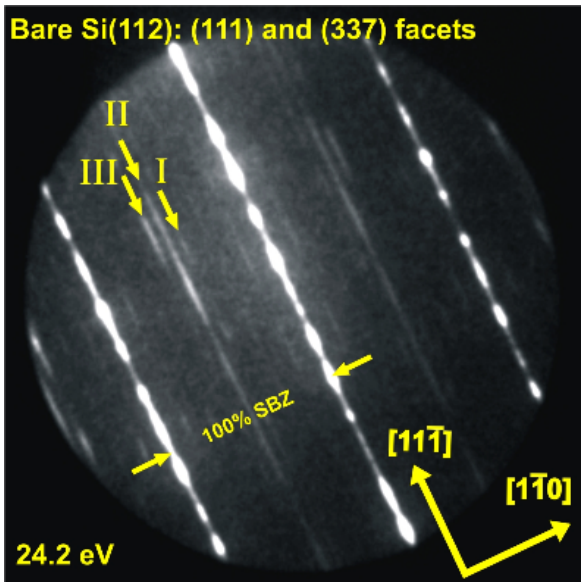

Figure 1. LEED pattern of the bare Si(112) surface. The image clearly reveals different $\frac{n}{7}$ order spots (the $\frac{3}{7}$ spots are indicated with I and the $\frac{4}{7}$ spots with III), that belong to the (7 × 7) reconstruction on the Si(111) facets, and $\frac{1}{2}$ order spots (indicated with II) along the $[11\bar{1}]$ direction, that belong to the (2 × 1) reconstruction on the (337) facets.

3.2. Ge island growth on Si(112)

Figure 2 shows *in situ* LEEM images during Ge deposition at a sample temperature of 590 °C with different Ge coverages Θ. On the bare surface (figure 2(a)) first a Ge wetting layer is formed (see figure 2(b)). After subsequent Ge deposition three-dimensional (3D) islands are observed (figure 2(c)). The island density increases rapidly (cf figures 2(c) and (d)) until it saturates (see figures 2(e) and (f)).

In figure 3 different bright-field LEEM images after Ge deposition with saturated Ge island density are displayed. The deposition temperature was varied between 420 °C in figure 3(a) and 590 °C in figures 3(e) and (f). At all growth temperatures the Ge islands exhibit a nearly circular shape, only at higher temperatures (see figures 3(e)) a slight shape anisotropy is visible. Similar to the growth on Si(111) [34, 35] and in sharp contrast to the Ge island growth on Si(113) [36, 37], no preferential growth direction can be seen. Further deposition beyond the stages shown here only results in larger island sizes, the island density stays unaffected. This underlines that the nucleation stage has been completed and subsequently deposited Ge can diffuse on the surface until it reaches an existing island. In this growth stage the diffusion length can be estimated from the island density.

Figure 4 shows the evolution of the Ge island density as a function of the growth temperature. In the range from 420 to 590 °C an Arrhenius-like behaviour is found. The slope of the fit is equal to an activation energy E_A = 2.06 eV. With this value and the following considerations the diffusion barrier height E_d can be estimated. According to nucleation theory by

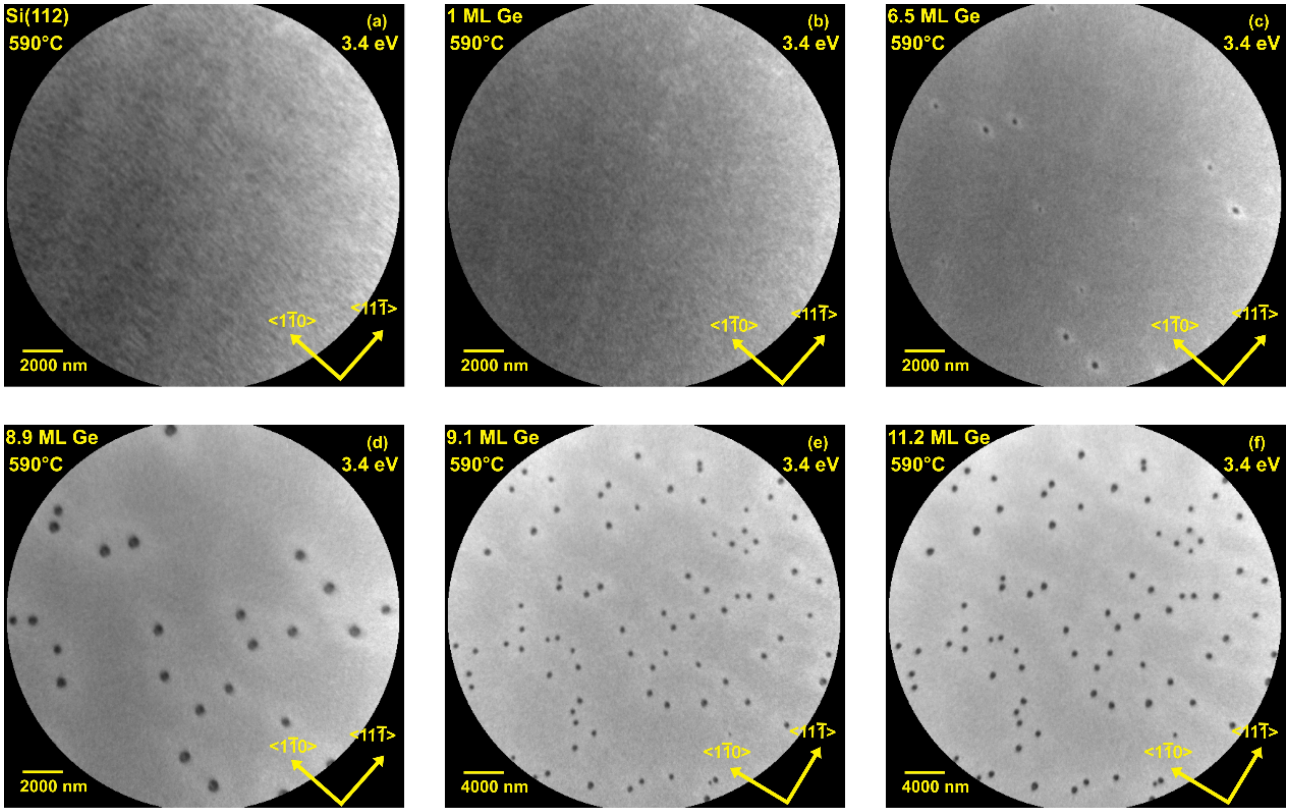

Figure 2. *In situ* bright-field LEEM images of Ge nanoislands on Si(112) during growth at 590 °C. In (a) the bare Si(112) surface with a preferential direction along [1$\bar{1}$0] is shown. At the initial stages of Ge deposition a wetting layer is formed (b). This can be seen by the fading of the contrast in this image. At higher Ge coverages 3D islands are formed (c)–(f), whose density increases quite rapidly up to a coverage of around 9 ML. The Ge coverages Θ and the electron energies are denoted in each frame. Note the larger field of view in (e) and (f).

Venables *et al* [38, 39] the island density is given by

$$N \sim \exp\left(\frac{E_c(i^*) + i^* E_d}{(i^*+2)k_B T}\right), \tag{1}$$

where i^* is the critical nucleus size and $E_c(i^*)$ the binding energy gained by the formation of a cluster with i^* atoms. In a first order approximation $E_c(i^*)$ is the covalent Ge–Ge bond energy E_b times the number n of additional covalent bonds within a cluster. For large clusters n is proportional to the number of atoms in the cluster:

$$E_c(i^*) \cong \alpha_{112} i^* E_b \tag{2}$$

with α_{112} being the average number of additional bonds per atom. From equations (1) and (2) the activation energy is determined as

$$E_A \cong \frac{i^*}{i^*+2}\left(\alpha_{112}E_b + E_d\right). \tag{3}$$

On Si(111) a critical nucleus size of $i^* \approx 6$ was reported [40] for Si homoepitaxy. As the Si(112) surface orientation is close to the Si(111) orientation and even consists partially of (111) facets the assumption of a large critical nucleus size can be justified in the present case. Since the Ge bond strength is much smaller compared to Si, an even larger critical nucleus size can be expected in our case. Hence, equation (3) can be approximated by

$$E_d \cong E_A - \alpha_{112}E_b. \tag{4}$$

With the heat of formation for Ge of around 291 kJ mol^{-1} [41] a value of $E_b = 1.51$ eV can be calculated. As the atomic structure of the Ge covered Si(112) surface is yet unknown we cannot determine the exact value for α_{112}. But because the (112) surface lies crystallographically between the (111) and (113) surface and is furthermore consisting partially of (111) facets, we assume α_{112} to be in the range of the values of α_{111} and α_{113} as well. For the (5×5) structure [28] on the Ge wetting layer on Si(111) the number of dangling bonds of the 25 Ge atoms per (5×5) unit cell reduces from 25 to nine, so $\alpha_{111} = 0.64$. For the eight atoms in the (2 × 2) structure [42] of the Ge wetting layer on Si(113) only two dangling bonds are left, resulting in $\alpha_{113} = 0.75$ [37]. Hence, $\alpha_{112} \approx 0.70$ is supposed. With this we obtain $E_d \approx 1.0$ eV for the diffusion barrier height[3]. This value is nearly twice as high as the value reported in [37] for the Ge growth on Si(113). This might be due to hindered diffusion across the facet boundaries.

[3] Taking into account the systematic error due to the approximation that leads from equation (3) to equation (4), i.e., the assumption of a virtually infinite critical nucleus size, as well as the uncertainty in the determination of α, we estimate a biased error bar of about +25% and −15% for the diffusion barrier heights given here.

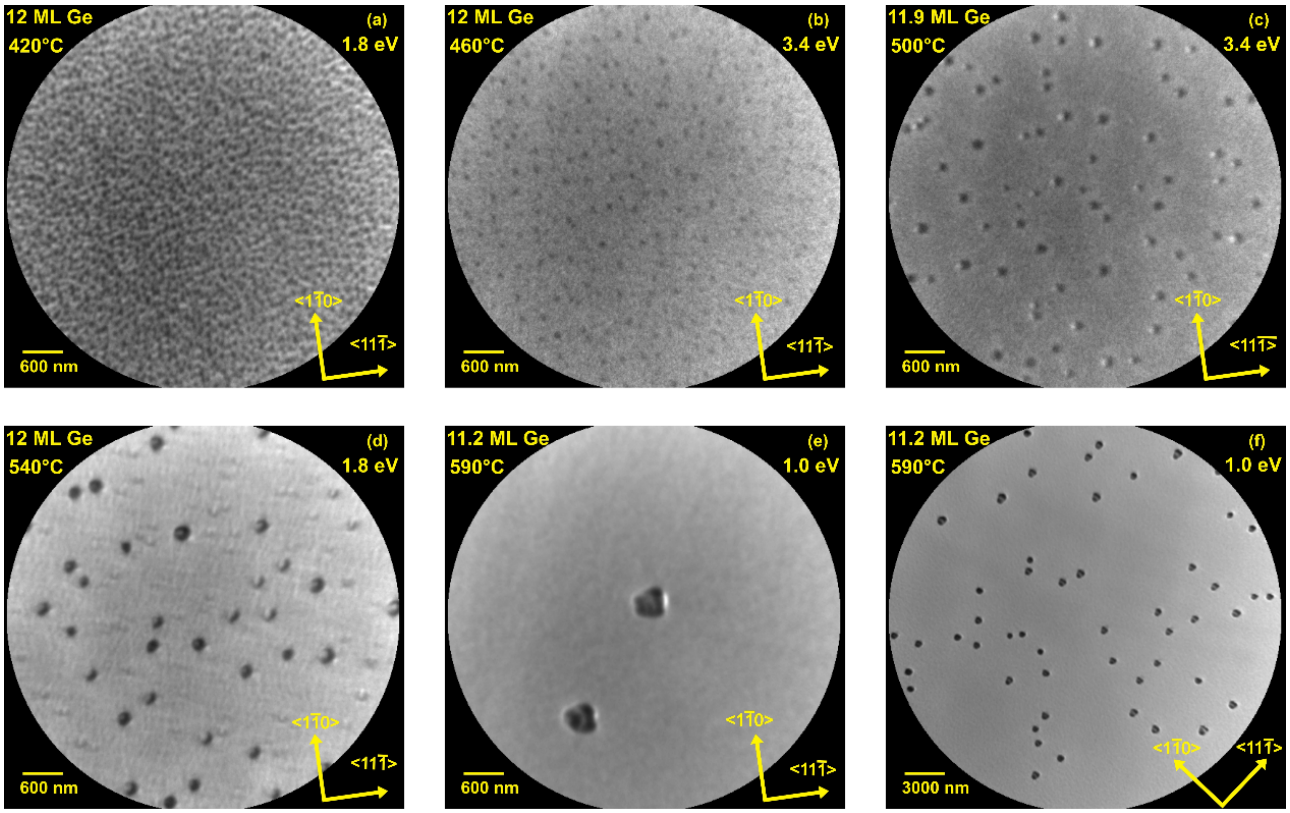

Figure 3. Bright-field LEEM images of Ge nanoislands on Si(112) surfaces for different growth temperatures. The island size increases with the temperature, whereas the island density N decreases. The Ge coverages Θ and the electron energies are denoted in each image. Note the larger field of view in (f).

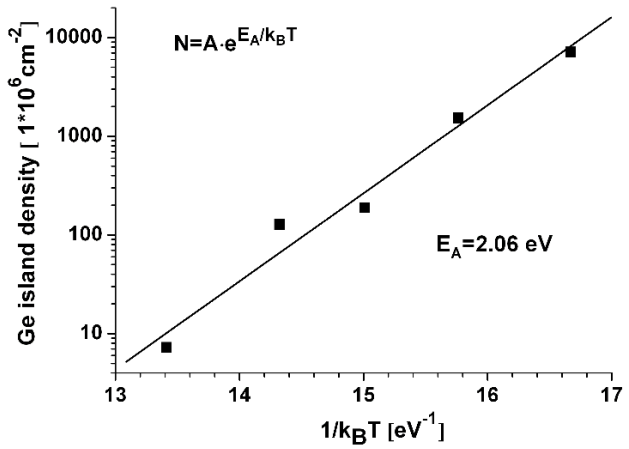

Figure 4. Growth temperature dependence of the Ge island density N on bare Si(112) in a range of 420–590 °C. The slope in the plot is equivalent to the activation energy E_A.

3.3. Ge island growth on Ga terminated Si(112)

Figure 5(a) shows a LEED image of the Ga covered Si(112) surface. We observe sharp LEED spots, indicating that the adsorption of Ga leads to a smoothening of the surface. Nevertheless, a few facet spots are still visible (see circles in figure 5(a)), showing that the surface is not completely defaceted. The vast majority of the surface area is terminated by a complex reconstruction that is connected to intense superstructure diffraction spots with a spot distance of 18% surface Brillouin zone (SBZ). This distance corresponds to an 'incommensurate (5.55 × 1)' reconstruction. From recent scanning tunnelling microscopy measurements (not shown here), it is revealed that this structure is not truly incommensurate but consists of a mixture of (5 × 1) and (6 × 1) building blocks. In core level spectroscopy (CLS) experiments we determined the saturation coverage to be 4.67×10^{14} atoms·cm^{-2}, which corresponds to (0.84±0.04) ML and confirms the proposed model for the (6 × 1) reconstruction as proposed by Snijders *et al* [22]. This model is further supported by our latest x-ray standing waves (XSW) experiments, where we were able to determine the two Ga adsorption sites to be one terrace and one step edge site. Both the CLS and the XSW data will be presented and discussed in a separate publication [43].

Deposition of several ML Ge onto the Ga/Si(112) system results in a (5 × 1) reconstructed surface with additional facet spots (see figure 5(b)). In contrast to the facet spots in figure 5(a) that have been attributed to remaining substrate facets, the facet spots in figure 5(b) are assigned to side facets of Ge 3D islands, as proven by the strong contrast in dark-field LEEM images (similar to the one shown in figure 7(c)). In additional X-PEEM (see figure 5(c)) images, where we used the Ge 3d signal for imaging, the Ge islands appear clearly bright (cf figure 5(c)).

Similar to the study of Ge growth on bare Si(112) we analysed the Ge deposition on the Ga terminated Si(112)

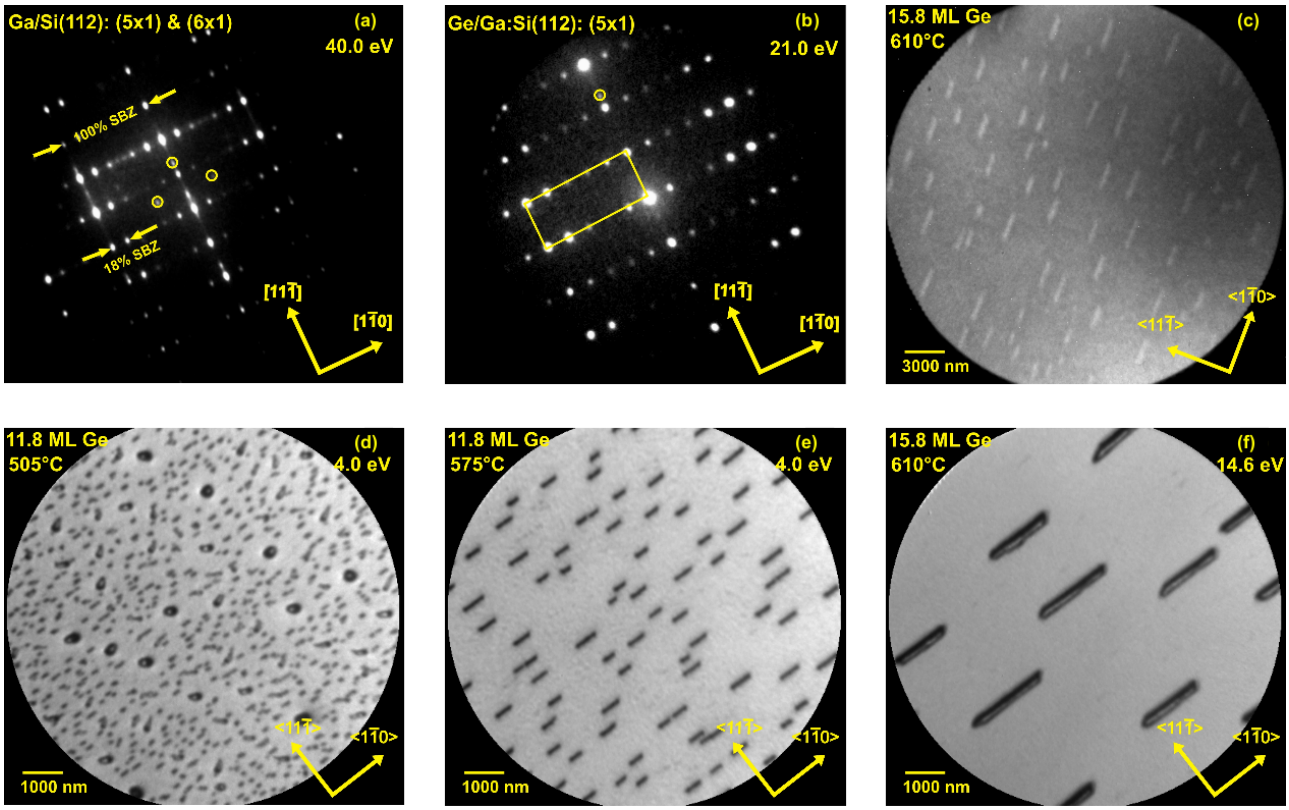

Figure 5. LEED patterns of the Ga terminated Si(112) surface (a) before and (b) after Ge island growth at 540 °C. The surface reconstruction in (a) is an 'incommensurate (5.55 × 1)' reconstruction, a mixture of (5 × 1) and (6 × 1) building blocks, with additional facet spots (see circles). In the LEED pattern in (b), a (5 × 1) reconstruction with additional facet spots is visible. These facet spots belong to Ge island facets. (c): X-PEEM image at a growth temperature of 610 °C; (d)–(f): bright-field LEEM images of Ge nanoislands on Ga terminated Si(112) for different growth temperatures between 505 and 610 °C. The island size increases with the temperature, whereas the island density N decreases. Note the larger field of view in the X-PEEM image in (c).

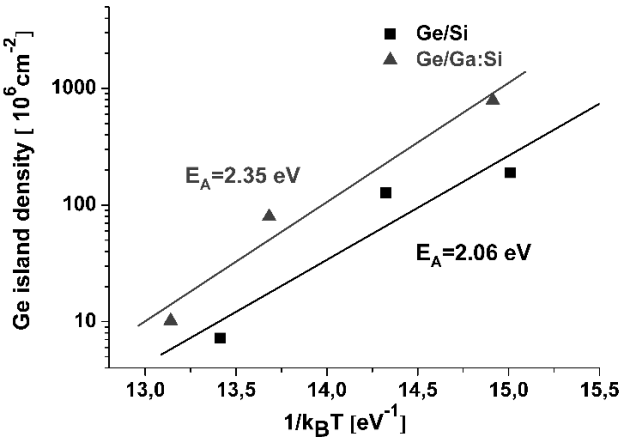

Figure 6. Comparison between the Arrhenius plots for the Ge island density N on bare (black) and on Ga terminated (grey) Si(112) in a range of 500–610 °C. The slopes in both plots are equivalent to the corresponding activation energies E_A.

surface at different growth temperatures between 505 and 610 °C. The resulting bright-field LEEM images are shown in figures 5(d)–(f). At the lowest growth temperature in figure 5(d) we observe slightly anisotropic islands with a bimodal size distribution, where there are denuded zones around the larger islands. A similar bifurcation of the size distribution was found for strained Ge islands on Si(001), which has been explained in terms of a change of the island chemical potential as a consequence of a strain induced shape transition [44]. In the present case, the observed surface morphology could likewise be explained by coarsening due to a more effective strain relaxation within larger Ge islands which, therefore, offer energetically more favourable incorporation sites as compared to smaller islands.

At higher growth temperatures the Ge islands exhibit a much more monodisperse size distribution and a pronounced anisotropy. The resulting Ge nanowires are elongated along the [1$\bar{1}$0] direction with a length of up to 2 μm and an aspect ratio of about 7:1 at a growth temperature of 610 °C (see figure 5(f)). This shape indicates a strong diffusion anisotropy and/or an anisotropic strain relaxation along the direction of the wires as compared to the perpendicular direction.

The temperature dependence of the Ge island density on the Ga terminated Si(112) surface is shown in figure 6, in comparison to the plot for the island density on the bare Si(112) surface. For all growth temperatures, the island density is significantly higher in case of Ga pre-adsorption. This can be attributed to a decreased Ge diffusion length due to the presence of surface Ga. Again an Arrhenius-like behaviour is found. Analogously to the procedure in the previous section

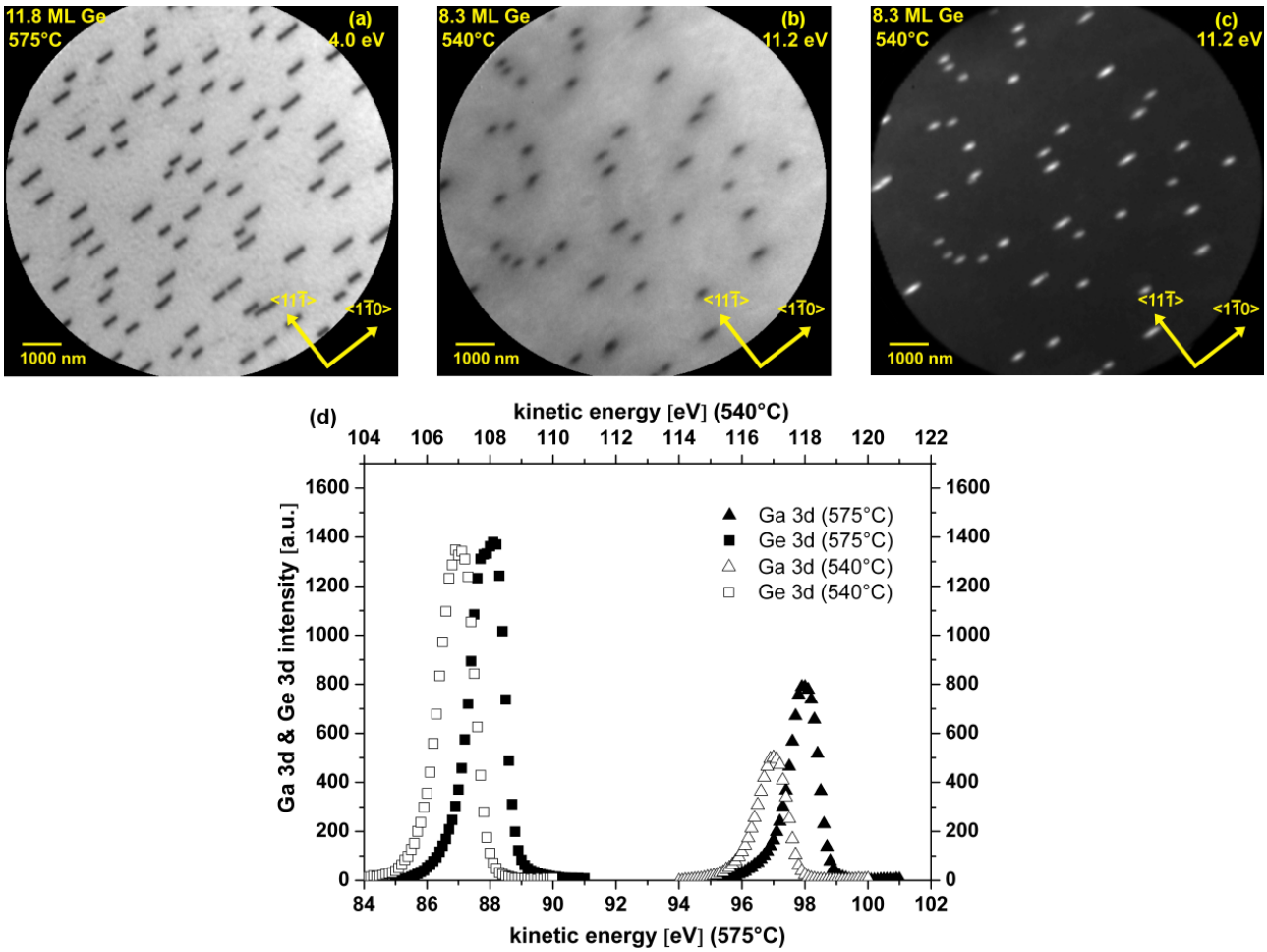

Figure 7. Bright-field LEEM images (a), (b) of Ge islands grown on Ga terminated Si(112) (a) with and (b) without Ga co-deposition during Ge growth. The dark-field LEEM image (c) shows the same area as the image in (b), but instead of the (00) spot one of the facet spots similar to the one in the LEED pattern in figure 5(b) was chosen, indicating that the facet spots belong to Ge island side facets. In (d) core level spectra of the samples in (a) and (b) are shown, indicating that for sample (b) a significant amount of Ga has desorbed from the surface. For better comparison the spectra of the sample in (b) were normalized so that both Ge spectra showed the same integrated intensity. Note that different kinetic energy scales apply for both samples, due to different photon energies used.

we determined the Ge diffusion barrier E_d to be about 1.3 eV (see footnote 1). The reduction of the Ge diffusion length in the presence of Ga is also supported by the data shown in figure 7. If Ge is grown at 540 °C with prior Ga pre-adsorption, but *without* Ga co-deposition during Ge growth, a significant amount of about 33% of the Ga is found to be desorbed, as determined from the CLS data in figure 7(d). As a consequence, the island density is strongly reduced, by a factor of about 5 as compared to the island density expected for Ge growth *with* Ga co-deposition at the same temperature.

4. Summary

In this study we analysed the Ge growth on Si(112) surfaces, both with and without Ga pre-adsorption. For both cases an Arrhenius-like behaviour of the Ge island density is found. Compared to Ge island growth on Si(113) [37] we found a much larger Ge diffusion barrier with a value of $E_d \approx 1.0$ eV, most likely due to hindered diffusion by the facets of the underlying substrate. Pre-adsorption of Ga leads to a decreased Ge diffusion length and thus to an enlarged diffusion barrier of about $E_d \approx 1.3$ eV. The Ge islands on the bare Si(112) exhibit a nearly circular shape over the whole temperature range and no preferential growth direction is found. In contrast to this, the Ge islands on the Ga terminated Si(112) surface show a strong anisotropy. We observe Ge nanowires with a length of up to 2 μm in [1$\bar{1}$0] direction and an aspect ratio of about 7:1. This shape suggests a strong diffusion anisotropy or an anisotropic strain relaxation that is not present for Ge island growth on the bare Si(112) surface.

Acknowledgments

This work has been supported by the Deutsche Forschungsgemeinschaft (Grant No. FA 363/6) and the physics international postgraduate (PIP) programme of the University of Bremen (supported by the German Academic Exchange Service). This research was carried out (in whole or in part) at the Center for Functional Nanomaterials, Brookhaven National Laboratory, which is supported by the US Department of Energy, Office

of Basic Energy Sciences, under Contract No. DE-AC02-98CH10886.

References

[1] Reinking D, Kammler M, Horn-von Hoegen M and Hofmann K R 1997 *Japan. J. Appl. Phys.* **36** L1082
[2] Konle J, Presting H, Kibbel H, Thinke K and Sauer R 2001 *Solid-State Electron.* **45** 1921
[3] Kanbe H, Komatsu M and Miyaji M 2006 *Japan. J. Appl. Phys.* **45** L644
[4] Kim H, Li H and Seo J M 2008 *Surf. Sci.* **602** 2563
[5] Maree P M J, Nakagawa K, Mulders F M, van der Veen J F and Kavanagh K L 1987 *Surf. Sci.* **191** 305
[6] LeGoues F K, Meyerson B S and Morar J F 1991 *Phys. Rev. Lett.* **66** 2903
[7] Copel M, Reuter M C, Kaxiras E and Tromp R M 1989 *Phys. Rev. Lett.* **63** 632
[8] Horn-von Hoegen M, LeGoues F K, Copel M, Reuter M C and Tromp R M 1991 *Phys. Rev. Lett.* **67** 1130
[9] Meyer G, Voigtländer B and Amer N M 1992 *Surf. Sci.* **274** L541
[10] Voigtländer B and Zinner A 1994 *J. Vac. Sci. Technol.* A **12** 1932
[11] Schmidt Th 1999 *Appl. Phys. Lett.* **74** 1391
[12] Schmidt Th, Kröger R, Clausen T, Falta J, Janzen A, Kammler M, Kury P, Zahl P and Horn-von Hoegen M 2005 *Appl. Phys. Lett.* **86** 111910
[13] Schmidt Th, Kröger R, Flege J I, Clausen T, Falta J, Janzen A, Zahl P, Kury P, Kammler M and Horn-von Hoegen M 2006 *Phys. Rev. Lett.* **96** 066101
[14] Falta J, Copel M, LeGoues F K and Tromp R M 1993 *Appl. Phys. Lett.* **62** 2962
[15] Schmidt Th, Flege J I, Gangopadhyay S, Clausen T, Locatelli A, Heun S and Falta J 2007 *Phys. Rev. Lett.* **98** 066104
[16] Schmidt Th, Clausen T, Flege J I, Gangopadhyay S, Locatelli A, Mentes T O, Guo F Z, Heun S and Falta J 2007 *New J. Phys.* **9** 392
[17] Fotiadis L and Kaplan R 1990 *Thin Solid Films* **184** 415
[18] Baski A A and Whitman L J 1995 *J. Vac. Sci. Technol.* A **13** 1469
[19] Jung T M, Prokes S M and Kaplan R 1993 *Surf. Sci. Lett.* **289** L577
[20] Baski A A, Erwin S C and Whitman L J 1999 *Surf. Sci. Lett.* **423** L265
[21] González C, Snijders P C, Ortega J, Pèrez R, Flores F, Rogge S and Weitering H H 2004 *Phys. Rev. Lett.* **93** 126106
[22] Snijders P C, Rogge S, González C, Pèrez R, Ortega J, Flores F and Weitering H H 2005 *Phys. Rev.* B **72** 125343
[23] Jung T M, Prokes S M and Kaplan R 1994 *J. Vac. Sci. Technol.* A **12** 1838
[24] Flege J I, Vescovo E, Nintzel G, Lewis L H, Hulbert S and Sutter P 2007 *Nucl. Methods Mat. Phys. Res.* B **261** 855
[25] Zahl P, Bierkandt M, Schröder S and Klust A 2003 *Rev. Sci. Instrum.* **74** 1222
[26] Patel J R, Freeland P E, Golovchenko J A, Kortan A R, Chadi D J and Qian G X 1986 *Phys. Rev. Lett.* **57** 3077
[27] Schmidt Th, Gangopadhyay S, Flege J I, Clausen T, Locatelli A, Heun S and Falta J 2005 *New J. Phys.* **7** 193
[28] Köhler U, Jusko O, Pietsch G, Müller B and Henzler M 1991 *Surf. Sci.* **248** 321
[29] Baski A A and Whitman L J 1995 *Phys. Rev. Lett.* **74** 956
[30] Baski A A and Whitman L J 1996 *J. Vac. Sci. Technol.* B **14** 992
[31] Zavitz D H, Evstigneeva A, Singh R, Fulk C and Trenary M 2005 *J. Electron. Mater.* **34** 839
[32] Takayanagi K, Tanishiro Y, Takahashi M and Takahashi S 1985 *J. Vac. Sci. Technol.* A **3** 1502
[33] Chuang F-C, Ciobanu C V, Wang C-Z and Ho K-M 2005 *J. Appl. Phys.* **98** 073507
[34] Sgarlata A, Szkutnik P D, Balzarotti A, Motta N and Rosei F 2003 *Appl. Phys. Lett.* **83** 4002
[35] Voigtländer B and Zinner A 1993 *Appl. Phys. Lett.* **63** 3055
[36] Omi H and Ogino T 1999 *Phys. Rev.* B **59** 7521
[37] Clausen T, Schmidt Th, Flege J I, Locatelli A, Mentes T O, Heun S, Guo F Z and Falta J 2006 *Appl. Surf. Sci.* **252** 5321
[38] Venables J A, Derrien J and Janssen A P 1980 *Surf. Sci.* **95** 411
[39] Venables J A, Spiller G D T and Hanbücken M 1984 *Rep. Prog. Phys.* **47** 399
[40] Voigtländer B, Zinner A, Weber T and Bonzel H P 1995 *Phys. Rev.* B **51** 7583
[41] *CRC Handbook of Chemistry and Physics* 1999 80th edn (New York: CRC Press)
[42] Zhang Z, Sumitomo K, Omi H, Ogino T, Nakamura J and Natori A 2002 *Phys. Rev. Lett.* **88** 256101
[43] Speckmann M *et al* 2009 in preparation
[44] Ross F M, Tersoff J and Tromp R M 1998 *Phys. Rev. Lett.* **80** 984